Cytoprotective Effects and Mechanisms of Δ-17 Fatty Acid Desaturase in Injured Human Umbilical Vein Endothelial Cells (HUVECs)

Authors' Contribution:
Study Design A
Data Collection B
Statistical Analysis C
Data Interpretation D
Manuscript Preparation E
Literature Search F
Funds Collection G

ABCDEFG **Haoyu Zhou**
ABCDEFG **Chengming Wang**

College of Food Science and Technology, Huazhong Agricultural University, Wuhan, Hubei, P.R. China

Corresponding Author: Chengming Wang, e-mail: chengmingwang1935@163.com
Source of support: Departmental sources

Background: The beneficial effect of Δ-17 FAD is poorly understood. The aim of this study was to investigate the protective mechanism of fatty acids against atherosclerotic (AS) damage induced by oxidized low-density lipoprotein (ox-LDL) in human umbilical vein endothelial cells (HUVECs), and to identify the molecular mechanisms involved.

Material/Methods: The ox-LDL was used to induce lipotoxicity in HUVECs to establish a model of oxidative injury. HUVECs were transfected with Δ-17FAD lentivirus to induce cytoprotective effects. We evaluated the alterations in cell proliferation and apoptosis, and oxidative stress index, including levels of nitric oxide (NO), malonyldialdehyde (MDA), SOD enzyme, LDH, GSH-PX, and vascular endothelial growth factor (VEGF) expression.

Results: The ox-LDL-induced excessive cellular apoptosis of HUVECs was abrogated by upregulation of Δ-17 FAD. Importantly, Δ-17 FAD converted ω-3 polyunsaturated fatty acid ARA into ω-6 polyunsaturated fatty acid EPA. Further, Δ-17 FAD overexpression promoted the proliferation of HUVECS, and inhibited ox-LDL-induced lipid peroxidation of HUVECs. The levels of nitric oxide, GSH-PX, and SOD enzyme were increased, and the activity of MDA and LDH was suppressed by the upregulation of Δ-17 FAD. In addition, upregulation of Δ-17 FAD significantly increased VEGF expression. *In vitro* tube formation assay showed that Δ-17 FAD significantly promoted angiogenesis.

Conclusions: These results suggest that Δ-17 fatty acid desaturase plays a beneficial role in the prevention of ox-LDL-induced cellular damage.

MeSH Keywords: **Atherosclerosis • Fatty Acid Desaturases • Human Umbilical Vein Endothelial Cells**

Full-text PDF: http://www.medscimonit.com/abstract/index/idArt/903654

📄 3667   ⊞ 1   📊 8   📚 41

Background

Cardiovascular disease, especially atherosclerosis (AS), has become the leading cause of death in adults. Endothelial injury induced by various factors may trigger early AS, leading to impaired endothelial function and reduced ability to regulate vascular function and homeostasis [1] Injury to endothelial cells is not only the initiating factor in the pathogenesis of AS, but is also a key factor in the activity of atherosclerotic plaque. Increased death of endothelial cells leads to arterial plaque, and accelerated renewal rate [2–4], further demonstrating that endothelial cell injury plays a decisive role in the development of atherosclerosis.

Oxidized low-density lipoprotein (ox-LDL) causes significant endothelial dysfunction resulting in adherence of macrophages, fibroblasts, and monocytes to the endothelium and migration into the endothelium [5,6]. The migrated cells form a large number of lipid-laden foam cells, eventually resulting in atherosclerotic plaques [7].

Saturated free fatty acids are the major inducers of endothelial cell apoptosis and inflammatory cytokines [8]. Free fatty acids (FFAS) are the main components of blood lipids, which affect the biological function of a variety of cells. High concentrations of FFAs induce apoptosis of pancreatic beta cells, ovarian granulosa cells, and testicular Leydig cells [9]. In humans, the enzyme stearoyl CoA desaturase 1 (SCD-1) is the limiting step in the synthesis of monounsaturated fatty acids, which protects endothelial cells against lipotoxicity [10]. Δ-17 fatty acid desaturase (FAD) shares 55% identity at the amino acid level with SCD-1 [11]. The beneficial effect of Δ-17 FAD is poorly understood. In this study, we tested the hypothesis that Δ-17 FAD abrogates ox-LDL-induced apoptosis in human umbilical vein endothelial cells (HUVECs), promotes HUVECs proliferation, and prevents lipotoxicity.

Material and Methods

Reagents

Δ-17 FAD: The original sequence of *Phytophthora ramorum* was obtained from NCBI: FW362214.1;
HUVEC cell line (American Type Culture Collection, Manassas, Virginia);
Lentiviral vector: pLV[Exp]-Neo (Cyagen);
Arachidonic acid and ox-LDL (Sigma-Aldrich, St. Louis, MO);
VEGF antibody (R&D Systems, Minneapolis, MN).

Δ-17 FAD codon optimization

Phytophthora ramorum Δ-17 FAD gene sequences were retrieved from NCBI (FW362214.1).

We accessed the website *http://www1kazusa1or1jp/codon/* to obtain the newest codon usage table, with preference codon amino acid sequence reverse translated into DNA sequence. We introduced cloning site Sma I and Kozak sequence, the sequence of stop codon changed to TGA (mammalian preference in the original sequence is TAA), the final sequence was synthesized and cloned into pUC vector (Nanjing Detai Biological Technology), and the sequence was to confirmed to be correct.

Lentiviral packaging

We used lentivirus gene expression vector (3rd generation) pLV[Exp]-NEO-EF1A, inserted the enhanced Green Fluorescent Protein EGFP and the ORF_1086bp* (Alias: DELTA-17), and the recombinant vector was named pLV[Exp]-EGFP/Neo-EF1A>ORF_1086bp*. We transfected 293T cells with assist plasmid for virus packaging, and after 48 h we collected the supernatant containing virus particles. The product of centrifuge filtering was stored at –80°C, and later used to determine the functional titer of the virus by fluorescence quantitative PCR.

HUVEC cell line culture

HUVEC cells were retrieved from the liquid nitrogen tank and quickly transferred into a 37°C water bath to thaw. After 1~2 min, the liquids in the vials were completely dissolved and the vials were transferred to a clean bench. After centrifugation at 1200 rpm for 5 min, the supernatant was aspirated and removed. We added 10 mL of RPMI-1640 medium supplemented with 10% fetal bovine serum (FBS) to the centrifuge tube to obtain a cell suspension. The cell suspension was transferred into the cell culture flasks and placed in a 37°C and 5% CO_2 incubator. Subcultures from passages 2–5 were selected for experimental use.

HUVEC cells infected with lentivirus

HUVECs were plated at a concentration of 1×10^5 cells in 6-well plate after overnight culture and infected at a Multiplicity of Infection (MOI) of 20 in the presence of polybrene (5 μg/mL) for 10 h. Infected cells were cultured for 48 h with 10% FBS medium. After 48 h of incubation, the cells were processed for further analysis.

Real-time PCR detection of lentivirus infection

Total RNA was extracted from HUVECs using a guanidine protocol. The extracted RNA was treated with DNase (RNase-free) to remove DNA contamination. RNA was quantified by measuring the absorbance at 260 nm, and the quality was checked with agarose gel electrophoresis. Four micrograms of RNA were reverse transcribed with oligo dT primers using M-MLV Reverse Transcriptase (MBI Fermentas) in a volume of

Table 1. Primers used in real-time PCR.

Primer	Name	Sequence
P1	FAD (forward primer)	5'-ACCAGTTCCCGACCCTGAC-3'
P2	FAD (reverse primer)	5'-TGCCCACCACGAAGTTGA-3'
P3	GAPDH (forward primer)	5'-GCACCGTCAAGGCTGAGAAC-3'
P4	GAPDH (reverse primer)	5'-TGGTGAAGACGCCAGTGGA-3'

20 mL. Primers were designed for *FAD* gene amplification, and the *GAPDH* gene was used as an internal standard (Table 1). Real-time RT-PCR was repeated 3 times for each sample. The PCR reaction system (20 μL) consisted of 10.5 μL dd H$_2$O, 0.5 μL Taq, 2 μL buffer, 2 μL 2.5 mmol/L dNTP, and 2 μL forward and reverse primers (10 μmol), respectively, and 1 μL template. The cycling parameters were 94ºC for 5 min, followed by 30 cycles of 94ºC for 30 s, 55ºC for 30 s, 72ºC for 30 s, and 72ºC for 10 min after 30 cycles. The expression of RACK1 and GAPDH was quantified according to the values derived from the standard curve (Ct).

Functional verification of Δ-17 FAD

Cells were harvested, and the total lipid was extracted by homogenization in chloroform/methanol (2: 1, vol/vol) containing 0.01% butylated hydroxyl toluene (Sigma, St. Louis, MO, USA) as antioxidant. Fatty acid methyl esters (FAMEs) were prepared, extracted, and purified by thin-layer chromatography (TLC) on a 20×20×0.25 mm silica gel 60 plate (Merck, Germany). FA profiles were analyzed using gas chromatography (GC–17A, Shimadzu, Kyoto, Japan) equipped with a 30×0.25 mm, 0.25 μm capillary column (VF–23 ms, Varian, Palo Alto, CA, USA) and a hydrogen flame ionization detector. The column was temperature-programed from 50°C to 170°C at a thermal gradient of 40°C/min and 170–230°C at 3°C/min. Both the detector and injection ports were set at 250ºC. Hydrogen served as a carrier gas at a flow rate of 1.1 mL/min. Individual methyl esters were identified by comparison with authentic FAs. The proportion of substrate FA converted to FA product was calculated from the gas chromatograms as 100×[Product Area/(Substrate Area + Product Area)].

Establishment of oxidative damage model

The experiment was composed of 7 subgroups, with each group from A to G representing the blank control, the negative control, the overexpression group (lentivirus-transfected), the ox-LDL group, the negative + ox -LDL group, the overexpression + arachidonic acid + ox-LDL group, and the overexpression + arachidonic acid group, respectively. To assess the concentration of ox-LDL, we processed cells with various concentrations of ox-LDL (20, 40, 60, 80, and 100 μg/mL) for a whole day. The decreased viability of ox-LDL cells is dose-dependent, and the viability of cells is reduced to 53.32±5.97% with the ox-LDL concentration of 80 μg/mL (data not shown). As a result, the following experiments still used the 80 μg/mL ox-LDL concentration standards.

Determination of cell proliferation

The passaged HUVECs suspension was centrifuged at 1200 rpm for 10 min. The supernatant was discarded and the sample was washed twice with balanced salt solution. After counting, the cell density was adjusted to 1×10^5/mL. The cells were seeded in a 96-well plate, diluted 1: 40 in the drug-containing serum with culture medium, and 0.1 mL was added into each well, with 3 compound wells for each group. The samples were placed in the 5% CO$_2$ cell incubator at 37°C for 48 h. The MTT solution was added to each well prior to measurement of absorbance at 490 nm.

Determination of apoptosis in HUVEC

To detect early stages of apoptosis, an Annexin-VFLUOS staining kit (Roche) was used according to the manufacturer's instructions. Briefly, HUVECs were washed with PBS and incubated with Annexin-V/propidium iodide (PI)/Hoechst 33342 for 15 min at room temperature. Cells were measured with flow cytometry (BD) and apoptosis was confirmed in Annexin-V-positive and PI-negative cells. The percentage of apoptotic cells was calculated by dividing Annexin-V-positive cells by the total number of cells visualized by Hoechst staining.

Effects of Δ-17 FAD on biochemical indices of SOD, GSH-Px, LDH, and MDA in HUVECs

Levels of NO, MDA, SOD, GSH-PX, and LDH were determined using specific enzyme-linked immunosorbent assay (ELISA) kits according to the manufacturer's instructions (Beyotime Institute of Biotechnology, Shanghai, China).

Western blot analysis of VEGF in HUVECs

Cells were lysed in RIPA buffer containing the protease inhibitor mixture (Roche). After incubation at 4°C for 30 min, soluble proteins were collected by centrifugation at 12 000 rpm for 15 min. Supernatants were analyzed for protein concentration with a Pierce protein assay kit and stored at –80°C. Proteins were separated on 10% SDS-polyacrylamide gel, and transferred to Immobilon-P membranes (Millipore). The filters were immunostained with rabbit monoclonal antibody against VEGF (1: 1000, R&D Systems) and antibody against β-actin (1: 1000, R&D Systems) as an internal control. The immunocomplexes were
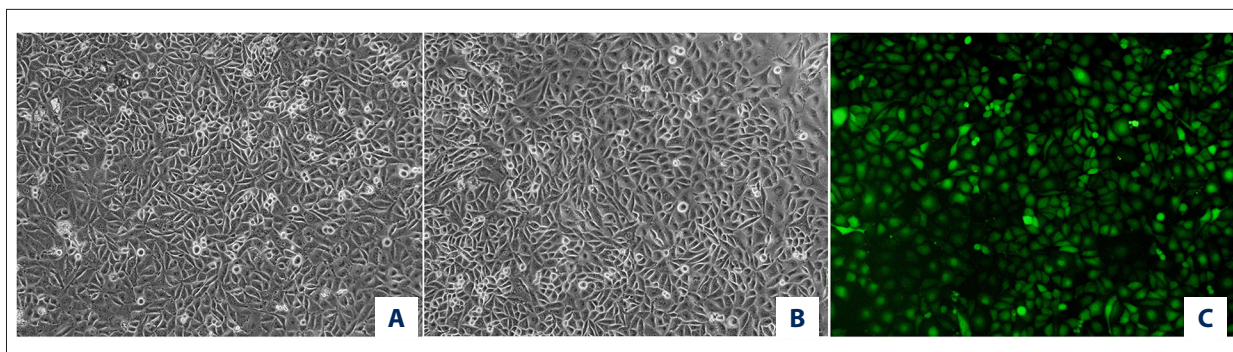
Figure 1. HUVECs under optical microscope (×100) (**A**) HUVECs passage 1; (**B**) HUVECs passage 5; (**C**) HUVECs infected by lentivirus for 48 h.
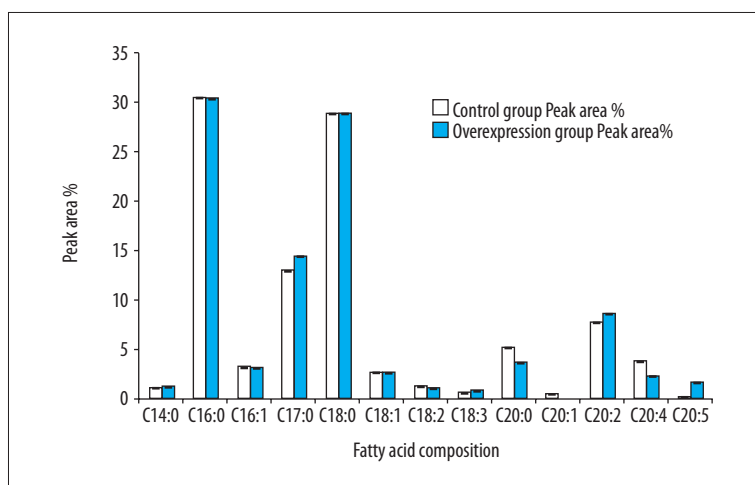

Figure 2. Fatty acid composition of HUVECs transfected with control and Δ-17 FAD.

detected with secondary antibody conjugated to horseradish peroxidase (1: 10,000, Santa Cruz Biotechnology) and visualized using the Immobilon™ Western Chemiluminescent Kit (Millipore).

Statistical analysis

Data are expressed as means ± SDs. Two treatment groups were compared by the unpaired Student's t-test and one-way ANOVA was performed for serial analysis. A value of $P<0.05$ was considered statistically significant.

Results

Efficacy of transduction

Primary HUVECs showed a cobblestone or pitching stone-like appearance with large dark nuclei, forming a confluent monolayer of cells after 2 to 3 days of culture (Figure 1A, 1B). The expression of GFP and cell transduction efficacy was assessed using fluorescence microscopy. Following the optimized transduction procedure, we found that 90% to 95% of cells showed GFP expression (Figure 1C).

RT-PCR of efficacy of lentivirus infection

We used GAPDH as the internal control to quantify the relative expression of the target gene *FAD*. As shown in Figure 2, the expression level of the overexpression group was significantly higher than in the control and negative control groups. The expression level in the ox-LDL group was significantly lower than in the other groups of cell dysfunction induced by ox-LDL (Figure 3).

Δ-17 FAD overexpression converts arachidonic acid to eicosapentaenoic acid

To confirm the normal function of 17 desaturase gene, omega -3 fatty acid desaturase was used in HUVECs. We used the changes in fatty acid levels of ARA-fed cells to analyze the total cellular lipids by gas chromatography (Figure 4). In the control group, the cells contained 12 types of fatty acids, including 3 monounsaturated fatty acids and 4 polyunsaturated fatty acids. In the overexpression group, the cells showed 12 different fatty acids, including 2 types of monounsaturated and 5 types of polyunsaturated fatty acids. The presence of Δ-17 FAD was substantially increased (413%) in EPA of
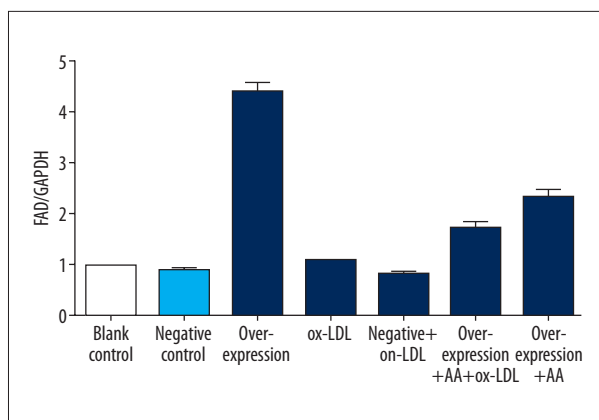
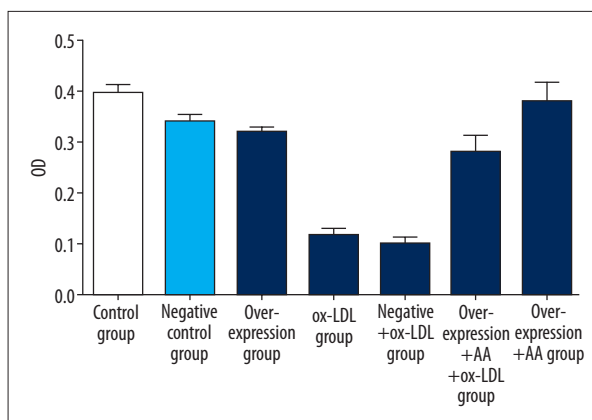**Figure 3.** The relative expression levels of FAD/GADPH in the different groups.

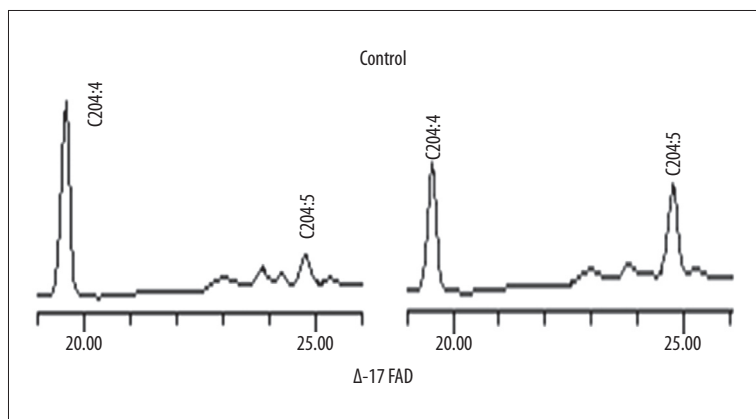**Figure 5.** Cell proliferation assay using MTT. Data represent means ±S.D.

Figure 4. Partial gas chromatogram traces showing fatty acid profiles of the total cellular lipids extracted from Δ17FAD-transformed HUVECs. Both the control and sΔ17FAD-transformed cells were fed with 0.05 mmol arachidonic acid for 48 h prior to fatty acid analysis. The lipid profiles show that the level of eicosapentaenoic acid (20: 5 n-3) was markedly increased and the level of arachidonic acid (20: 4 n-6) was significantly decreased in Δ17FAD-transformed cells compared with the control cells (asterisks represent $p < 0.05$).

HUVECs. EPA was up to 0.339% in the control cells and up to 1.742% in the overexpressing cells ($p < 0.05$, Figure 2). In contrast, the level of ARA substrate was reduced from 3.953% in the control cells to 2.374% in the transformed cells, which is a reduction of 39.94% ($p < 0.05$), and the ARA/EPA rate was reduced from 11.661% to 1.363%. No change was observed in the composition of other fatty acids between the control and transformed cells.

Determination of cell proliferation using MTT

Compared with the control group, the cell viability in the negative and the overexpression groups slightly decreased. The cell viability of the ox-LDL and the negative + ox-LDL groups was significantly decreased compared with the control group ($P < 0.05$ and $P < 0.01$, respectively). The overexpression of FAD reversed the decrease in ox-LDL-induced cell viability, especially in the overexpression + arachidonic acid group ($p < 0.01$) (Figure 5).

Determination of cellular apoptosis with flow cytometry

Compared with the control group, the ox-LDL group showed a large number of apoptotic cells. The apoptosis index (AI) in the ox-LDL group was significantly higher than in the control and the overexpression groups ($P < 0.01$). The apoptosis rate was 0.1%, 64.9%, and 67.1% for the control, the ox-LDL, and the negative + ox-LDL groups, respectively. It was significantly decreased in the overexpression group, the overexpression + ox-LDL + arachidonic acid group, and the overexpression + arachidonic acid group, which were 12.8%, 12.4%, and 3.8%, respectively (Figure 6).

Effects of Δ-17 FAD on biochemical indices of SOD, GSH-Px, LDH, and MDA in HUVECs

After ox-LDL treatment of HUVECs, the NO content decreased from 4.5 μmol/mL in the control group to 1.25 μmol/mL and 0.66 μmol/mL in the ox-LDL and the negative + ox-LDL groups, respectively. It increased from 4.5 μmol/mL in the control group to 12.25 μmol/mL, 4.55 μmol/mL, and 12.23 μmol/mL in the overexpression group, the overexpression + ox-LDL +
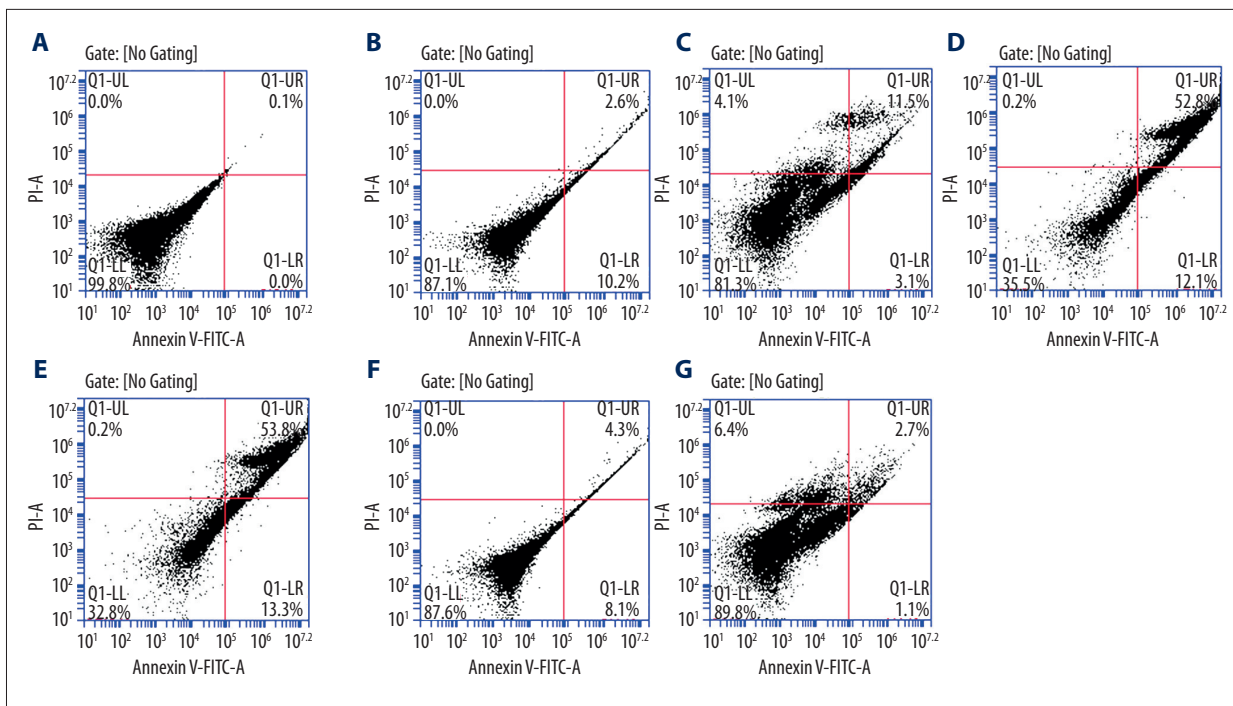
Figure 6. Cellular apoptosis assay using flow cytometry. (**A**) blank control group; (**B**) negative control group; (**C**) overexpression group; (**D**) ox-LDL group; (**E**) negative + ox -LDL group; (**F**) overexpression + arachidonic acid + ox-LDL group; and (**G**) overexpression + arachidonic acid group.

Figure 7. NO, MAD, SOD, GSH-PX, and LDL assays using ELISA. Data represent means ±S.D. (**A**) NO content, (**B**) MAD content, (**C**) SOD activity, (**D**) GSH-PX activity, (**E**) LDL activity.

arachidonic acid group, and the overexpression + arachidonic acid group, respectively (Figure 7A).

After ox-LDL treatment of HUVECs, the MAD content significantly increased from 5.67 μmol/mL in the control group to 13.43 μmol/mL and 13.01 μmol/mL in the ox-LDL group and the negative + ox-LDL group, respectively. It decreased from 5.67 μmol/mL in the control group to 1.74 μmol/mL, 5.97μmol/

mL, and 1.83 μmol/mL in the overexpression group, the overexpression + ox-LDL + arachidonic acid group, and the overexpression + arachidonic acid group, respectively (Figure 7B).

After ox-LDL treatment of HUVECs, the SOD activity was significantly decreased from 1.41U in the control group to 0.44 U and 0.45 U in the ox-LDL group and the negative + ox-LDL group, respectively. It increased from 1.41 U in the control group to

Figure 8. Expression of VEGF in the 7 groups as determined by Western blot analysis. (**A**) blank control group; (**B**) negative control group; (**C**) overexpression group; (**D**) ox-LDL group; (**E**) negative + ox -LDL group; (**F**) overexpression + arachidonic acid + ox-LDL group; and (**G**) overexpression + arachidonic acid group.
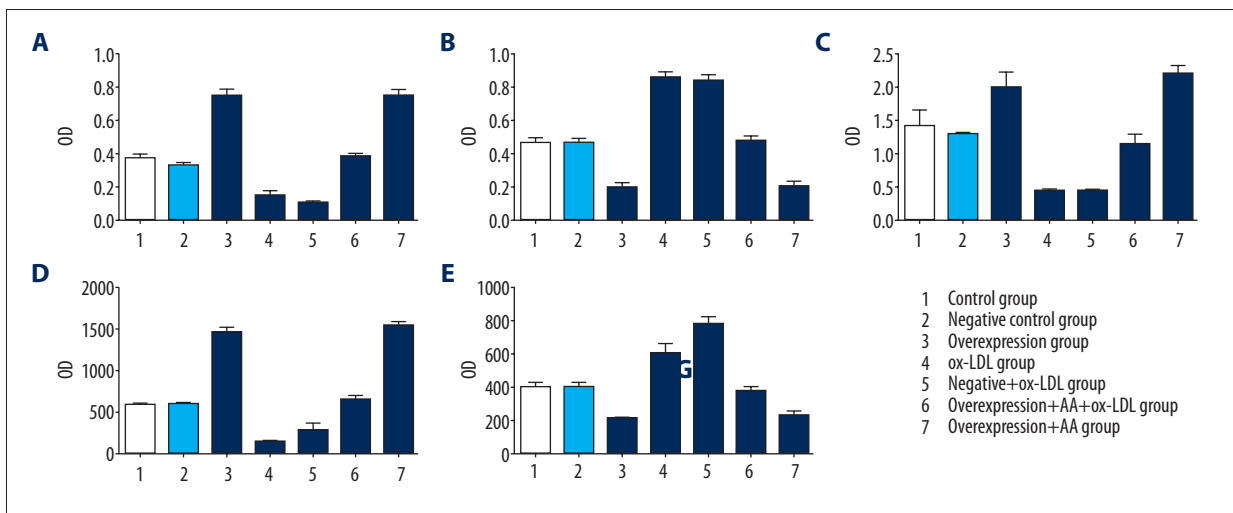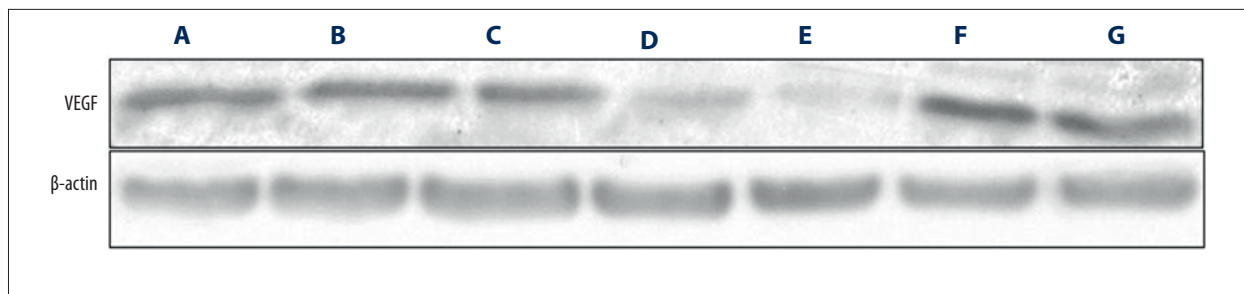
2 U, 1.15 U, and 2.2 U in the overexpression group, the overexpression + ox-LDL + arachidonic acid group, and the overexpression + arachidonic acid group, respectively (Figure 7C).

Following ox-LDL treatment of HUVECs, the GSH-PX activity significantly decreased from 587 mU/mg in the control group to 132.9 mU/mg and 278.6 mU/mg in the ox-LDL group and the negative + ox-LDL group, respectively. It increased from 587 mU/mg in the control group to 1466 mU/mg, 587 mU/mg, and 1552 mU/mg in the overexpression group, the overexpression + ox-LDL + arachidonic acid group, and the overexpression + arachidonic acid group, respectively (Figure 7D).

After ox-LDL treatment of HUVECs, the LDH activity was significantly increased from 414 U/L in the control group to 610 U/L and 786 U/L in the ox-LDL group and the negative + ox-LDL group, respectively. It decreased from 414 U/L in the control group to 216 U/L, 388 U/L, and 234 U/L in the overexpression group, the overexpression + ox-LDL + arachidonic acid group, and the overexpression + arachidonic acid group, respectively (Figure 7E).

Western blot analysis of VEGF in HUVECs

As shown in Figure 8, ox-LDL suppressed the expression of VEGF by HUVECs. In contrast, Δ-17 FAD increased ox-LDL-inhibited VEGF expression, suggesting that any inhibition of VEGF expression is regulated by Δ-17 FAD.

Discussion

Cardiovascular and cerebrovascular diseases are among the most prevalent diseases worldwide, with devastating health consequences, and atherosclerosis is the pathological basis of these diseases. Inflammation and endothelial cell injury contribute to atherogenesis. Recent evidence also associated endothelial injury with monocyte and platelet adhesion, aggregation, and release of cytokines and platelet-derived growth factor at sites in the arterial wall containing endothelial cell desquamation [12]. Among the several detrimental factors, ox-LDLs, the

principal cholesterol-carrying lipoproteins of the plasma, participate in the formation and progression of lesions by triggering lipid storage, local inflammation, and toxic events, leading to endothelial cell injury and death, plaque transition from stable to vulnerable, erosion and frank rupture, and subsequent atherothrombosis [13]. Cohort studies suggest an association between ox-LDL and cardiovascular events via atherosclerotic plaque formation and disruption [14,15]. It is believed that ox-LDL induces leukocyte activation and inflammatory responses triggering cell degranulation, phagocytosis of apoptotic cells, and, eventually, cardiovascular tissue damage [16].

The main risk factors of AS include damage to the intima of the artery and formation of atherosclerotic plaque. Injury to arterial intima is a functional disorder or anatomic injury. Intimal thickening is a component of AS pathogenesis [17,18]. Elevated levels of free fatty acid (FFAS) may alter endothelial basement membrane permeability. Foam cells easily penetrate into the arterial intima, leading to intimal thickening. Simultaneously, non-essential fatty acids (NEFA) increase the gene expression of amino GP, exacerbating AS [19]. Zhan [20] found that saturated fatty acids PA and SA and monounsaturated fatty acid OA exerted strong toxic effects against vascular endothelial cells. Polyunsaturated fatty acids partially blocked the vascular endothelial cell death induced by PA, which protected the endothelial cells. SCD-1 catalyzes the limiting step in the desaturation of saturated fatty acids to monounsaturated fatty acids (MUFAs), which plays a beneficial role in endothelial cell protection against lipotoxicity [21]. SCD-1 plays an anti-AS role in animal models (22). Δ-17 FAD, a newly identified FAD, shares 55% identity at the amino acid level with SCD-1 [10,11]. Since SCD-1 plays a beneficial role protecting endothelial cells against lipotoxicity, we postulated that Δ-17 FAD also plays a key role in endothelial cell function. Christon [23] fed obese rats with polyunsaturated fatty acids (c20: 5) and found that endothelial function of obese rats fed with fish oil (C20: 5) was significantly improved compared with the control group of obese rats not exposed to fish oil. The protective effect of polyunsaturated fatty acids was mediated via inhibition of the expression of adhesion molecules or improved

production of nitric oxide. The redox state of the endothelial cell membrane prevented the activation of endothelial cells. This study showed that FAD17 exerted a protective effect on the endothelial cells, similar to the results of Christon.

Oxidative damage and endothelial dysfunction are significant factors underlying the initiation and progression of atherosclerosis. Zhang et al. [24] demonstrated that ox-LDL decreased HUVEC viability by inducing cellular inflammation and apoptosis in a dose-dependent manner. In the present study, we found that ox-LDL significantly inhibited HUVEC viability. The overexpression of Δ-17 FAD reversed the decrease in ox-LDL-induced cell viability (Figure 5). Ox-LDL-induced apoptosis in vascular endothelial cells represents the pathophysiological basis of atherosclerosis [25,26]. In this study, we demonstrated the protective effect of Δ-17 FAD against ox-LDL-induced apoptosis in HUVECs (Figure 6A–6G). Further studies are needed to clarify the mechanisms underlying the protective effects of Δ-17 FAD against endothelial cell apoptosis.

During physiological and pathological processes, the human body often produces free radicals, which are subsequently removed by antioxidant systems, including superoxide dismutase (SOD), glutathione peroxidase (GSH-PX), glutathione transferase enzymes, and other enzymes, as well as glutathione (GSH), vitamin C, vitamin E, uric acid, β-carotene, and ceruloplasmin. SOD and GSH-PX are the major free radical scavenging enzymes [27–29]. Disruption of the dynamic equilibrium between oxygen free radicals and antioxidant systems leads to excessive production of oxygen or reduced clearance of free radicals. Combined with decreased antioxidant capacity of SOD, this results in a significant increase in malondialdehyde (MDA) content, triggering further cell damage, cellular metabolic dysfunction, cell death, and tissue damage via decomposition of lipid hydroperoxide [30,31]. Therefore, MDA levels may reflect the degree of lipid peroxidation in the body. In the present study, we demonstrated that ox-LDL significantly decreased SOD and GSH-PX, and increased MDA content by HUVECs. The overexpression of Δ-17 FAD abrogated the oxidative damage induced by ox-LDL (Figure 7B–7D).

Nitric oxide (NO) is an important bioactive substance produced from L-arginine via NO synthase in endothelial cells [32,33]. NO inhibits platelet and monocyte-macrophage adhesion and endothelial cells, and smooth muscle cell proliferation [34,35]. ox-LDL acts on HUVECs to reduce NO synthesis by suppressing NO synthase activity, leading to cell adhesion, proliferation, and blood vessel contraction [36]. In the present study, we demonstrated the protective effect of Δ-17 FAD on ox-LDL-induced reduction of NO in HUVECs (Figure 7A). Further, we showed that the overexpression ofΔ-17 FAD abrogated ox-LDL-induced release of LDL by HUVECs (Figure 7E). These results suggest that Δ-17 FAD partially reversed ox-LDL-induced oxidative damage

in endothelial cells. This may be due to the role 17FAD plays in ω3 fatty acid desaturase, which is able to convert the ω6 arachidonic acid to the ω-3 eicosapentaenoic acid with high substrate conversion efficiency. Many fundamental research and clinical studies have shown that ω3 polyunsaturated fatty acids can inhibit oxidative stress and inflammatory reaction and is beneficial in the prevention of cardiovascular disease [37–39]. Eicosapentaenoic acid (EPA) and DHA are both involved in cardiovascular protection; they can modify several risk factors for the development of atherosclerosis, such as total cholesterol, high levels of plasma triglyceride, low levels of plasma HDL cholesterol, high aggregability of platelets, and leukocyte and monocyte reactivity. Several of these effects may be mediated through changes in prostanoid formation, such as by competitive inhibition of production of arachidonic acid-derived thromboxane A2 (TXA2) and prostacyclin (PGI2) or by increased production of EPA-derived prostanoids (TXA3 and PGI3). Also, EPA can inhibit adverse cholesterol effects, reduce the deposition in the vascular wall, and can assist the high-density lipoprotein cholesterol (HDL) in clearing the vascular wall. Therefore, EPA not only reduces blood lipids, but also prevents the occurrence of coronary heart disease and cerebrovascular disease.

Lee et al. [40] demonstrated that VEGF secreted by endothelial cells is critical for endothelial cell survival and maintenance of homeostasis. The vast majority of VEGF-knockout mice exhibit internal bleeding, thrombosis, and other symptoms, suggesting the role of VEGF in maintaining vascular integrity. VEGF regulates endothelial cell growth and differentiation, and is also an endothelial cell mitotic agent. Research on the mechanism of VEGF in the apoptosis of vascular endothelial cells [41] showed that VEGF could inhibit the apoptosis of HUVEC induced by ox-LDL and TNF-α via downregulating Fas mRNA expression and upregulating Bcl-2 mRNA expression. Our study shows that the ox-LDL group had inhibited expression of VEGF, while the expression of VEGF was increased in the overexpression + arachidonic acid + ox-LDL group and the overexpression + arachidonic acid group. Our results show that Δ17 FAD can induce anti-oxidative stress, enhance the expression of VEGF to increase cell survival rate, inhibit cell apoptosis, and exhibits a protective effect against oxidative damage of HUVECs induced by ox-LDL (Figure 8).

Conclusions

Our study demonstrated that Δ-17 FAD protects endothelial cells against oxidative damage induced by ox-LDL. Therefore, Δ-17 FAD is a potential therapeutic agent in the prevention and treatment of atherosclerosis. Furthermore, our results provide a basis for the potential application of Δ-17 *FAD* gene in the production of transgenic livestock to synthesize essential ω3 PUFAs, or animal models to investigate syndromes caused by the lack of EPA.

References:

1. Wang JC, Bennett M: Aging and atherosclerosis: Mechanisms, functional consequences, and potential therapeutics for cellular senescence. Circ Res, 2012; 111: 245–59

2. Pavel P, Mateja KJO: Markers of preclinical atherosclerosis and their clinical relevance. Vasa, 2015; 44: 247–56

3. Gräfe M, Steinheider G, Desaga U et al: Characterization of two distinct mechanisms for induction of apoptosis in human vascular endothelial cells. Clin Chem Lab Med, 1999; 37: 505–10

4. Vizzardi E, Gavazzoni M, Della PP et al: Noninvasive assessment of endothelial function: The classic methods and the new peripheral arterial tonometry. J Investig Med, 2014; 62: 856–64

5. Di PN, Formoso G, Pandolfi A: Physiology and pathophysiology of oxLDL uptake by vascular wall cells in atherosclerosis. Vascul Pharmacol, 2016; 84: 1–7

6. Trpkovic A, Resanovic I, Stanimirovic J et al: Oxidized low-density lipoprotein as a biomarker of cardiovascular diseases. Crit Rev Clin Lab Sci, 2015; 52: 1–16

7. Rafieian-Kopaei M, Setorki M, Doudi M et al: Atherosclerosis: Process, indicators, risk factors and new hopes. Int J Prev Med, 2014; 5: 927–46

8. Ishida T, Naoe S, Nakakuki M et al: Eicosapentaenoic acid prevents saturated fatty acid-induced vascular endothelial dysfunction: Involvement of long-chain acyl-CoA synthetase. J Atheroscler Thromb 2015; 22: 1172–85

9. Mu YM, Yanase T, Nishi Y et al: Saturated FFAs, palmitic acid and stearic acid, induce apoptosis in human granulosa cells. Endocrinol, 2001; 142: 3590–97

10. Chiara S, Melania G, Fabrizia C, Amalia G: The subtle balance between lipolysis and lipogenesis: A critical point in metabolic homeostasis. Nutrients, 2015; 7: 9453–74

11. Xue Z, He H, Hollerbach D et al: Identification and characterization of new Δ-17 fatty acid desaturases. Appl Microbiol Biotechnol, 2013; 97: 1973–85

12. Morrell CN, Aggrey AA, Chapman LM, Modjeski KL: Emerging roles for platelets as immune and inflammatory cells. Blood, 2014; 123: 2759–67

13. Napoli C. Oxidation of LDL, atherogenesis, and apoptosis. Ann NY Acad Sci, 2003; 1010: 698–709

14. Di Pietro N, Formoso G, Pandolfi A: Physiology and pathophysiology of ox-LDL uptake by vascular wall cells in atherosclerosis. Vascul Pharmacol, 2016; 84: 1–7

15. Santilli F, D'Ardes D, Davì G: Oxidative stress in chronic vascular disease: From prediction to prevention. Vascul Pharmacol, 2015; 74: 23–37

16. Al-Banna N, Lehmann C: Oxidized LDL and LOX-1 in experimental sepsis. Mediators Inflamm, 2013; 2013: 761789

17. Feher M, Elkeles R: Lipid modification and coronary heart disease in type 2 diabetes: Different from the general population? Heart, 1999; 81: 10–11

18. Ziouzenkova O, Perrey S, Asatryan L et al: Lipolysis of triglyceride-rich lipoproteins generates PPAR ligands: Evidence for an antiinflammatory role for lipoprotein lipase. Proc Natl Acad Sci, 2003; 100: 2730–35

19. Miller AL, Plane F, Jeremy JY et al: Delayed recovery of receptor-mediated functional responses to acetylcholine in mouse isolated carotid arteries following endothelial denudation *in vivo*. J Vasc Res, 2003; 40: 449–59

20. Nandy D, Johnson C, Basu R et al: The effect of liraglutide on endothelial function in patients with type 2 diabetes. Diab Vasc Dis Res, 2014; 11: 419–30

21. Sampath H, Ntambi JM: The role of stearoyl-CoA desaturase in obesity, insulin resistance, and inflammation. Ann NY Acad Sci, 2011; 1243: 47–53

22. Brown JM, Chung S, Sawyer JK et al: Inhibition of stearoyl-coenzyme A desaturase 1 dissociates insulin resistance and obesity from atherosclerosis. Circ, 2008; 118: 1467–75

23. Christon RA: Mechanisms of action of dietary fatty acids in regulating the activation of vascular endothelial cells during atherogenesis. Nutr Rev, 2003; 61: 272–79

24. Zhang Y, Mu Q, Zhou Z et al: Protective effect of irisin on atherosclerosis via suppressing oxidized low density lipoprotein induced vascular inflammation and endothelial dysfunction. PLoS One, 2016; 11: e0158038

25. Hong D, Bai Y-P, Gao H-C et al: Ox-LDL induces endothelial cell apoptosis via the LOX-1-dependent endoplasmic reticulum stress pathway. Atheroscler, 2014; 235: 310–17

26. Ding Z, Liu S, Sun C et al: Concentration polarization of ox-LDL activates autophagy and apoptosis via regulating LOX-1expression. Sci Rep 2013; 3: 2091

27. Rahman T, Hosen I, Islam MT, Shekhar HU: Oxidative stress and human health. Adv Biosci Biotechnol, 2012; 3: 997

28. Rajendran P, Nandakumar N, Rengarajan T et al: Antioxidants and human diseases. Clin Chim Acta, 2014; 436: 332–47

29. Rosenfeldt F, Wilson M, Lee G et al: Oxidative stress in surgery in an ageing population: Pathophysiology and therapy. Exp Gerontol, 2013; 48: 45–54

30. Tarr M, Samson F. Oxygen free radicals in tissue damage: Springer Science & Business Media; 2013

31. Apostolova N, Victor VM: Molecular strategies for targeting antioxidants to mitochondria: Therapeutic implications. Antioxid Redox Signal, 2015; 22: 686–729

32. Förstermann U, Sessa WC: Nitric oxide synthases: regulation and function. Eur Heart J, 2012; 33: 829–37

33. Tousoulis D, Kampoli A-M, Tentolouris Nikolaos Papageorgiou C, Stefanadis C: The role of nitric oxide on endothelial function. Curr Vasc Pharmacol, 2012; 10: 4–18

34. Li H, Horke S, Förstermann U: Vascular oxidative stress, nitric oxide and atherosclerosis. Atherosclerosis, 2014; 237: 208–19

35. Fenyo IM, Gafencu AV: The involvement of the monocytes/macrophages in chronic inflammation associated with atherosclerosis. Immunobiology, 2013; 218: 1376–84

36. Davidson SM, Duchen MR: Endothelial mitochondria contributing to vascular function and disease. Circ Res, 2007; 100: 1128–41

37. JMJ Lamers, LMA Sassen, JM Hartog et al: Dietary N-3 polyunsaturated fatty acids and ischemic heart disease. Subcellular Basis of Contractile Failure, 1990; 237–56

38. Weiner BH, Ockene IS, Levine PH et al: Inhibition of atherosclerosis by cod-liver oil in a hyperlipidemic swine model. N Engl J Med, 1986; 315: 841–46

39. Nelson GJ, Schmidt PC, Corash L: The effect of a salmon diet on blood clotting, platelet aggregation and fatty acids in normal adult men. Lipids, 1991; 26(2): 87–96

40. Lee S, Chen TT, Barber CL et al: Autocrine VEGF signaling is required for vascular homeostasis. Cell, 2007; 130: 691–703

41. Cheng Y: The effect and mechanical study of vascular endothelial growth factor on the apoptosis of vascular endothelial cell. Huazhong University of Science and Technology, 2007